Detection of the inflammatory process in a Behçet's disease-like mouse model using ^{18}F-fluorodeoxyglucose positron emission tomography

S.B. Cho[1], S. Sohn[2], Z. Zheng[1], A. Cho[3], H. Kim[4], W.J. Kang[3], D. Bang[1], M. Yun[3], J.D. Lee[3], J.H. Lee[3]

[1]Department of Dermatology and Cutaneous Biology Research Institute, Yonsei University College of Medicine, Seoul, Korea; [2]Laboratory of Cell Biology, Ajou University Institute for Medical Sciences, Suwon, Korea; [3]Department of Nuclear Medicine, Yonsei University College of Medicine, Seoul, Korea; [4]Department of Pathology, Yonsei University College of Medicine, Seoul, Korea.

**Sung Bin Cho, MD, PhD*
**Seonghyang Sohn, PhD*
Zhenlong Zheng, MD, PhD
Arthur Cho, MD
Hyunki Kim, MD, PhD
Won Jun Kang, MD, PhD
Dongsik Bang, MD, PhD
Mijin Yun, MD, PhD
Jong Doo Lee, MD, PhD
Jae-Hoon Lee, MD

**These authors contributed equally to this work.*

Please address correspondence to:
Jae-Hoon Lee, MD,
Department of Nuclear Medicine,
Yonsei University College of Medicine,
50 Yonsei-ro, Seodaemun-gu,
120-752 Seoul, Korea.
E-mail: docnuke@yuhs.ac

Received on February 19, 2013; accepted in revised form on April 4, 2013.

Clin Exp Rheumatol 2013; 31 (Suppl. 77): S47-S53.

Key words: Behçet's disease, ^{18}F-fluorodeoxyglucose positron emission tomography, Behçet's disease-like mouse model, inflammation

Funding: this study was supported by a grant from the Korea Healthcare Technology R&D Project, Ministry of Health and Welfare, Republic of Korea (A110488).

Competing interests: none declared.

ABSTRACT

Objectives. *The major role of herpes simplex virus (HSV) type 1 infection in Behçet's disease (BD) immunopathogenesis has been demonstrated and inoculating the earlobes of ICR mice with HSV produced a BD-like mouse model. ^{18}F-fluorodeoxyglucose positron emission tomography (FDG PET) is widely used for diagnosing numerous human diseases other than malignancies. The aim of our study was to evaluate the inflammatory activities of BD-like symptoms in a HSV type 1-induced BD-like mouse model by small-animal FDG PET.*

Methods. *Five HSV-infected ICR mice with BD-like lesions, two asymptomatic HSV-infected mice, and two untreated mice were scanned with microPET, and autopsy specimens were histopathologically assessed to evaluate for infiltration by mixed inflammatory cells.*

Results. *The histopathological evaluation of the inflammatory process in knee and elbow joints significantly correlated with the quantitative assessment of FDG accumulation in the same joints in BD-like ICR mice, HSV-infected asymptomatic mice, and untreated control mice. Small-animal FDG PET clearly detected asymptomatic joint inflammatory processes in both BD-like mice and HSV-infected asymptomatic mice. In addition, genital ulcers and skin ulcers with associated perilesional lymphadenopathies in BD-like models were detected by microPET. However, biodistributed PET-positive images from the stasis of secreted FDG into the bowel lumen could not be distinguished from the inflammatory bowel lesions of BD when compared to FDG uptake in control mice.*

Conclusion. *Our data indicate that FDG PET can non-invasively and quantitatively detect the inflammatory process in an HSV-induced BD-like mouse model.*

Introduction

Behçet's disease (BD) is a chronic, multisystem vasculitis that theoretically affects all sizes and types of blood vessels (1). Although pathogenesis remains enigmatic, the major role of viral infection in BD immunopathogenesis, especially herpes simplex virus (HSV) type 1 infection, has been demonstrated in several reports (2-6). HSV type 1 has been significantly detected in saliva, intestinal ulcers, and genital ulcers by polymerase chain reaction in BD patients compared with healthy controls (3, 4). In addition, inoculating the earlobes of ICR mice with HSV produced a BD-like mouse model, and HSV DNA sequences were detected in the cutaneous and gastrointestinal ulcerative lesions of this mouse model (7). Although pretreatment or concurrent treatment of HSV-inoculated ICR mice with famciclovir could not prevent the development of BD-like symptoms, famciclovir seemed to be effective in improving BD-like symptoms and preventing recurrence in the symptomatic BD-like mouse model (8).

^{18}F-fluorodeoxyglucose positron emission tomography (FDG PET) is widely used for diagnosing numerous human diseases other than malignancies, including various causes of arthritis and vascular disease. However, to date, there have been few reports describing the clinical efficacy of FDG PET in BD patients (9-14). According to previous reports, FDG PET imaging is not believed to be effective for the detection of white-matter lesions in patients with neuro-BD (9, 10). In regard to vascular diseases affecting major arteries, Denecke *et al*. reported the inflammatory activity of pulmonary artery aneurysms detected by FDG PET in patients with BD (11). Our study group also reported eight BD patients presenting remark-

able FDG uptake in the cardiovascular lesions associated with BD, including aneurysms, pseudoaneurysms, aortitis, and arteritis (12). In addition, FDG uptake in orogenital ulcerative mucosal lesions, joint lesions, and erythema nodosum-like skin lesions have been demonstrated in BD patients (13, 14). In this report, we investigate the characteristics of FDG uptake in the inflammatory activities of BD-like lesions in a BD-like mouse model using small-animal PET compared with untreated ICR mice and asymptomatic HSV-infected ICR mice as controls.

Table I. Clinical characteristics of symptomatic Behçet's disease-like mice.

Clinical findings	Symptomatic Behçet's disease-like mice				
	1	2	3	4	5
Oral ulcers	–	–	–	–	–
Genital ulcers	–	–	–	+	–
Skin lesions	+	–	+	–	+
Eye lesions	–	+	–	–	+
Vascular involvement	–	–	–	–	–
Arthritis	–	–	–	–	–
CNS involvement	–	–	–	–	–
GI involvement	–	+	–	–	–

CNS: central nervous system; GI: gastrointestinal system.

Materials and methods

Behçet's disease-like mouse model

As described previously (7), 4–5-week-old male ICR mice were infected with HSV type 1 (1 X 10^6 plaque forming unit/ml, F strain), which was grown in Vero cells. The earlobes of the mice were scratched with a needle, and the virus inoculation was performed twice with a 10-day interval, followed by 16 weeks of observation. Mice were bred in temperature- and light-controlled conventional rooms (20–22°C, 12-hour light cycle starting at 8:00 a.m.) with free access to food and water.

Among the clinical manifestations in human BD patients, mouth ulceration, genital ulceration, erythema, skin pustules, skin ulceration, arthritis, diarrhea, red eye or reduced vision, loss of balance, and discolouration and swelling of the face were considered BD-like symptoms in the mouse model (7, 8). Mice with at least one major symptom were selected as having BD. The clinical characteristics of symptomatic BD-like mice (n=5) are summarised in Table I. Both untreated ICR mice (n=2) and asymptomatic ICR mice infected with HSV type 1 (n=2) were used as controls. Our experimental protocols were approved by the animal care committee of the Ajou University School of Medicine (Suwon, Korea).

^{18}F-fluorodeoxyglucose positron emission tomography

MicroPET (Inveon Dedicated PET; Siemens Medical Solutions, Malvern, PA, USA) was used in this study for FDG PET imaging and has an approximate resolution of 1.65±0.06 mm full-width-at-half-maximum (15, 16). Briefly, a PET scan was performed approximately 60 minutes after the intravenous injection of 7.8±0.42 MBq (212±11.3 μCi) FDG in 200 ml of phosphate buffered saline (PBS) via a tail vein. During the periods of injection, accumulation, and scanning, the mice were anesthetised under 2% isoflurane and kept warm using a heating pad to maintain a body temperature of 37°C.

Acquired PET data were reconstructed with the 3-dimensional maximum a posteriori (MAP) reconstruction algorithm, and no attenuation correction was applied. The microPET images were analysed using the AsiPro software (Siemens Medical Solutions). Skin ulcers were visually assessed, and volumes of interest (VOIs) were manually drawn on the skin ulcers and any suspicious hypermetabolic foci in the BD-like mouse and used to measure the tissue uptake of the glucose analogue. In addition, VOIs were applied to all of the elbow and knee joints in both BD-like mice and controls. FDG uptake of the inflammatory tissues was measured as percentage of injected dose per gram (%ID/g).

Histopathology

Immediately after performing FDG PET scans, mice were sacrificed, and tissue samples, including ulcerative skin lesions, both elbow and knee joints regardless of their symptoms, and the ileocecal portion of the intestine, were obtained and fixed. Then, a pathologist evaluated the sections with haematoxylin-eosin staining. In all cases, infiltrative mixed inflammatory cells were counted using the specimens obtained from joint tissues at a x200 magnification in 3–6 fields, and values are expressed as mean cell number. In addition, central nervous system involvement of BD was ruled out in all of the BD-like mice and controls by clinical manifestations and pathologic evaluation of brain tissues (17).

Statistical analysis

Values for quantitative variables are described as the mean and standard deviation. Spearman's rank correlation coefficients were used to ascertain whether the quantitative uptake index of FDG PET was associated with the inflammatory cell infiltration. All of the analyses were performed using SAS software version 9.2 (SAS Institute Inc., Cary, NC, USA). A *p*-value less than 0.05 was considered statistically significant.

Results

^{18}F-fluorodeoxyglucose uptake and joint inflammation

Histopathological assessment of inflammatory cell infiltration into the synovial membranes and perisynovial fat tissues of elbow and knee joints was performed for quantitative scoring of articular inflammation of the experimental ICR mice (Table II, Fig. 1). Symptoms suggestive of BD-related arthritis and/or arthralgia were not present in any of the BD-like mouse model or controls, except for secondary gait disturbance in one BD-like mouse with extensive cutaneous ulceration (case 3) and one BD-like mouse presenting

Table II. Quantitative analysis of joint inflammation in the Behçet's disease (BD)-like mouse model.

Mouse	Elbow joint (right/left)						Knee joint (right/left)					
	Maximum FDG uptake*		Mean FDG uptake*		Mean inflammatory cell count		Maximum FDG uptake*		Mean FDG uptake*		Mean inflammatory cell count	
BD-like mouse 1	5.0	5.1	3.0	3.5	53	59	9.9	10.1	4.3	4.7	142	175
BD-like mouse 2	0.6	0.5	0.4	0.3	41	136	1.2	1.2	0.4	0.4	75	42
BD-like mouse 3	3.0	12.0	2.4	6.6	57	189	9.6	7.8	4.2	4.2	154	93
BD-like mouse 4	5.4	5.4	3.2	3.2	65	96	15.1	20.5	8.6	9.7	188	184
BD-like mouse 5	4.3	5.4	2.2	2.9	73	37	8.2	8.6	3.2	3.2	62	97
HSV-infected control mouse 1	10.3	8.8	5.9	4.4	102	62	20.5	17.6	11.7	11.7	110	139
HSV-infected control mouse 2	19.7	19.7	11.8	13.8	160	127	31.5	33.5	17.7	21.6	148	256
Control mouse 1	3.7	2.6	1.2	1.2	30	16	5.8	2.9	3.8	1.9	52	9
Control mouse 2	2.9	2.6	1.9	1.8	14	8	2.6	4.1	1.8	3.0	8	11

*Values are expressed as percentage of injected dose per gram; FDG: ^{18}F-fluorodeoxyglucose; HSV: herpes simplex virus.

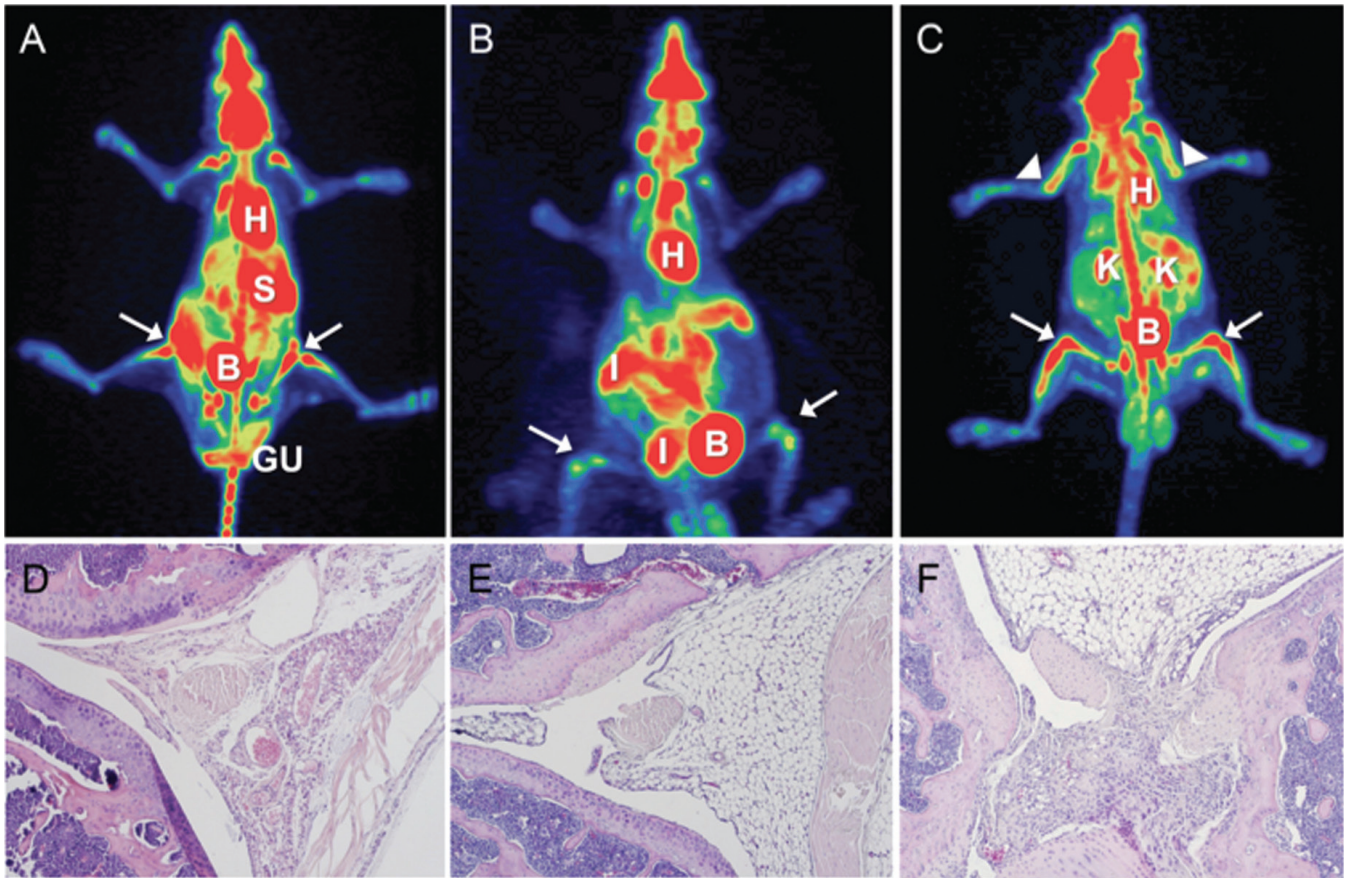

Fig. 1. ^{18}F-fluorodeoxyglucose (FDG) positron emission tomography (PET) and histopathology of joint inflammation. (**A**) A BD-like mouse (case 4) with focal FDG uptake in the knee joints (arrows). (**B**) A BD-like mouse (case 2) without noticeable FDG uptake suggestive of joint inflammation in the knee joints (arrows). (**C**) An asymptomatic herpes simplex virus (HSV)-infected mouse (case 2) with focal FDG uptake in the elbow (arrowheads) and knee joints (arrows). Histopathologic features of left knee joints in BD-like mice (**D**; case 4 and **E**; case 2) and (**F**) an asymptomatic HSV-infected mouse (case 2); haematoxylin and eosin stain with original magnification x100. B: bladder; GU: genital ulceration; H: heart; I: intestine; K: kidney; S: stomach.

with genital ulceration with excessive bleeding (case 4).

In the five BD-like mice, the mean number of inflammatory cells in the knee joint region was 121.2±53.9 cells, whereas control mice presented an inflammatory cell count of 163.3±63.9 in asymptomatic HSV-infected ICR mice and 20±21.4 in untreated ICR mice. In addition, the elbow joint region revealed a mean inflammatory cell count of 80.6±47.9, whereas the mean cell count was measured as 112.8±41.3 in asymptomatic HSV-infected ICR mice and 17±9.3 in untreated ICR mice.

In the five BD-like mice, the maximum and mean percentages of injected-FDG activity in the knee joint region

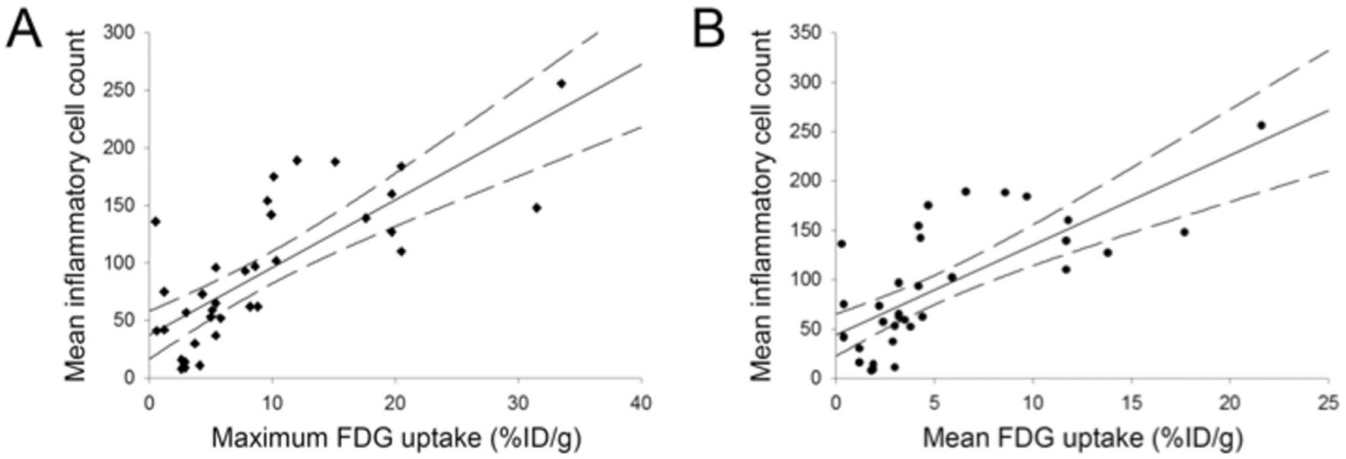

Fig. 2. Correlation of joint inflammation and ^{18}F-fluorodeoxyglucose (FDG) uptake in the Behçet's disease (BD)-like mouse model and controls. (**A**) Correlation between maximum FDG uptake and mean inflammatory cell count. (**B**) Correlation between mean FDG uptake and mean inflammatory cell count. Trend lines were inserted by linear regression analysis with 95% confidence intervals (dotted lines) using the SigmaPlot 2000 ver. 6.0 (SPSS Inc., Chicago, IL, USA). %ID/g: percentage of injected dose per gram.

were 9.2±5.7 and 4.3±3.0, respectively. Control mice presented maximum and mean % ID/g values of 25.8±7.9 and 15.7±4.9, respectively, in asymptomatic HSV-infected ICR mice and 3.9±1.5 and 2.6±1.0, respectively, in untreated ICR mice. In addition, the elbow joint region revealed maximum and mean % ID/g values of 4.7±3.2 and 2.8±1.8, respectively, whereas FDG accumulation was measured as 14.6±5.9% ID/g and 9.0±4.5% ID/g, respectively, in asymptomatic HSV-infected ICR mice and 3.0±0.5% ID/g and 1.5±0.4% ID/g, respectively, in untreated ICR mice.

Histopathological evaluation of the inflammatory process in the knee joint region significantly correlated with the quantitative assessment of FDG accumulation in the same joints in BD-like ICR mice, HSV-infected asymptomatic mice, and untreated control mice (maximum FDG uptake, r=0.843, p<0.0001; mean FDG uptake, r=0.811, p<0.0001; Fig. 2). In addition, the elbow joint region showed significant correlation between the histopathological assessment of infiltrated inflammatory cell counts and quantitative PET results in identical joint regions in BD-like ICR mice, HSV-infected asymptomatic mice, and untreated control mice (maximum FDG uptake,

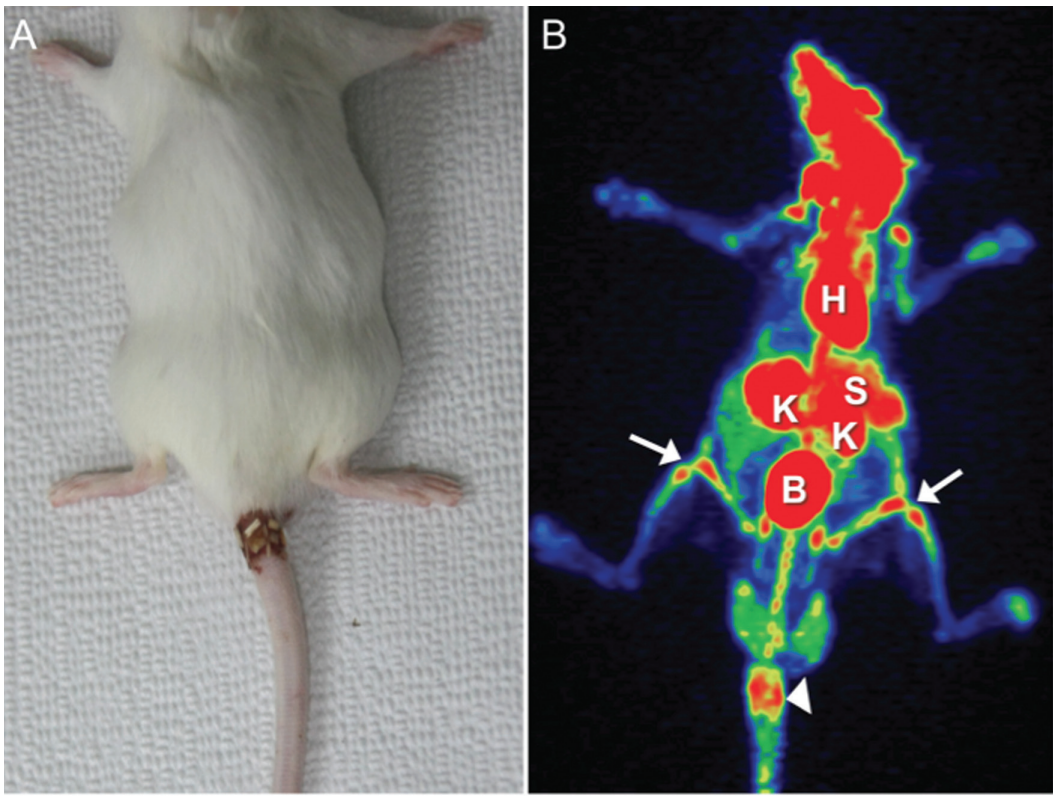

Fig. 3. (**A**) Herpes simplex virus-induced Behçet's disease-like mouse with tail ulceration (case 1), and (**B**) FDG uptake is increased around both knee joints (arrows) and the tail lesion (arrowhead). B: bladder; H: heart; K: kidney; S: stomach.

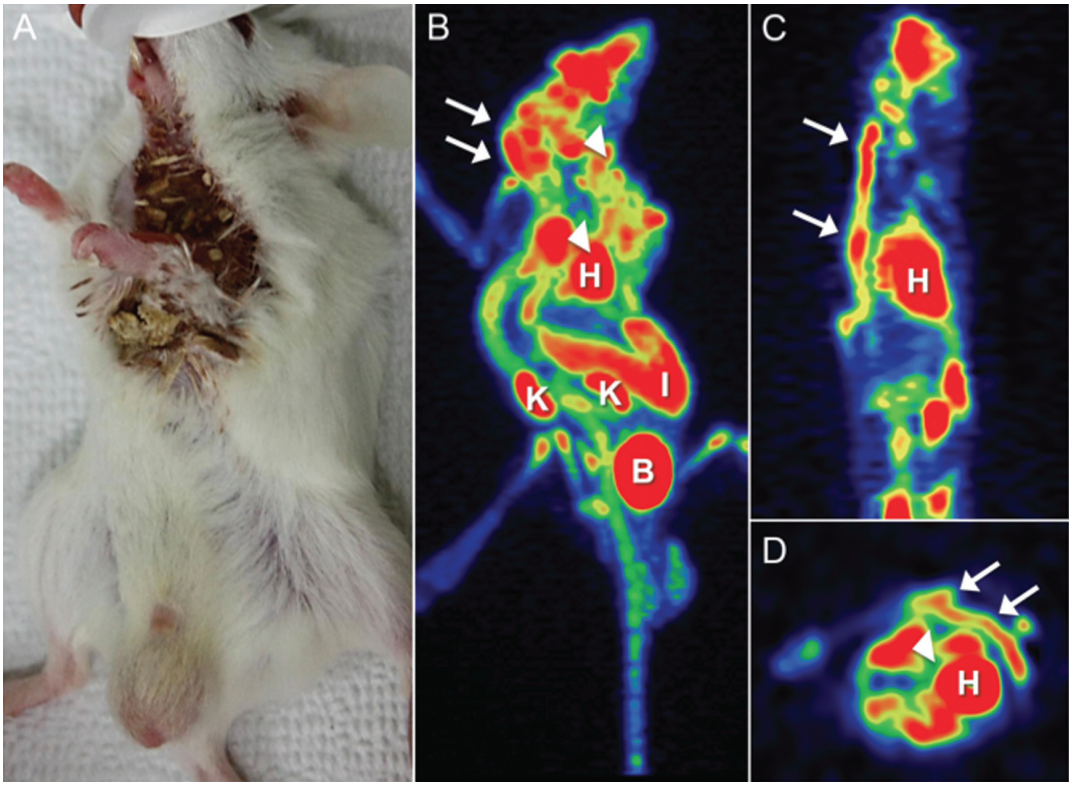

Fig. 4. (**A**) Herpes simplex virus-induced Behçet's disease-like mouse with extensive cutaneous ulceration (case 3), and (B-D) ^{18}F-fluorodeoxyglucose (FDG) positron emission tomography (**B**, maximum intensity projection view; **C**, sagittal view; **D**, axial view). Focal ^{18}F-fluorodeoxyglucose (FDG) uptake on the skin ulceration (arrows) and perilesional lymphadenopathies (arrowheads). B: bladder; H: heart; I: intestine; K: kidney.

r=0.769, p=0.0013; mean FDG uptake, r=0.722, p=0.0036).

Case 1

A male ICR mouse which was infected with HSV type 1 presented the BD-like symptom of skin ulceration on the tail (Fig. 3A). After the acquisition of PET data from whole body microPET, tissue samples were obtained from the tail and both elbow and knee joints. Focal FDG uptake was detected in the ulcerative skin lesion on the tail, and diffuse uptake was identified in both knee joints, suggestive of arthritis (Fig. 3B). The mean mixed inflammatory cell count in the tail ulceration was 154 cells at a x200 magnification, and maximum FDG accumulation was measured as 9.8% ID/g.

Case 2

A male HSV-infected ICR mouse demonstrated the BD-like symptoms of red eyes and abdominal distension. After microPET analysis, the BD-like mouse was autopsied, and a markedly distended, strangulated intestine without clinical signs of intestinal ischaemia was found. Tissue samples were obtained from the intestine with strangulation and both elbow and knee joints. On FDG PET images, distended bowel loops appeared as photophenic areas in the abdomen, and multifocal FDG uptake foci were noted in the right mid and lower portions of the abdomen. However, biodistributed PET-positive images from the stasis of secreted FDG into the bowel lumen could not be distinguished from the inflammatory bowel lesions of BD when compared to FDG uptake in the control mice.

Case 3

A BD-like ICR mouse presented extensive cutaneous ulceration involving nearly the entire chest wall, neck, and left arm (Fig. 4A). After the acquisition of PET data from whole body microPET, tissue samples were obtained from the ulcerative skin lesions and both elbow and knee joints. Multifocal FDG uptake was detected in the ulcerative skin lesions as well as lymph nodes of the neck and chest (Fig. 4B). The mean mixed inflammatory cell count in the chest ulceration was 235 cells at a x200 magnification, and the maximum FDG accumulation was measured as 16.6% ID/g. Massive infiltration of inflammatory cells was found in the left elbow joint with remarkable FDG uptake; however, it was suggested that the infiltrated cells originated from the extensive adjacent skin ulceration.

Case 4

A male HSV-infected ICR mouse presented with genital ulceration. After having microPET analysis, the BD-like mouse was autopsied, and the specimens obtained from the PET-positive ulcerative lesion were revealed to have extensive mixed inflammatory cell infiltration. The mean mixed inflammatory cell count in the genital ulceration was 174 cells at a x200 magnification, and the maximum FDG accumulation was measured as 13.0% ID/g (Fig. 1A).

Case 5

A BD-like ICR mouse presented with a left red eye and periocular and periauricular skin ulcerations. MicroPET demonstrated focal FDG uptake in the periocular and periauricular areas, which clinically presented as skin ulcers. The mean mixed inflammatory cell count in the periauricular skin ulceration was 112 cells at a x200 magnification, and the maximum FDG accumulation was measured as 11.6% ID/g.

Discussion

BD involves multiple organs with symptomatic heterogeneity (18, 19). In addition, pathognomonic laboratory findings and imaging modalities for baseline workup to detect systemic inflammatory reactions have not been established either in BD patients or in BD-like animal models (3, 20). Until recently, animal studies using BD-like models have been investigated mostly by methods that score BD severity, such as the BD activity index, and through analysis of autopsy specimens (7, 8, 21). However, current clinical scoring or histopathologic analysis methods have limitations when performing *in vivo* or longitudinal quantitative experiments with a relatively small number of animals (22).

In the present study, we investigated an *in vivo* imaging modality for visualisation and quantification of the inflammatory process in an HSV-induced BD-like mouse model using small-animal PET. Because joint involvement of BD usually presents clinically as intermittent and self-limiting monoarticular or oligoarticular arthritis and histopathologically as non-erosive arthritis, we evaluated both elbow and knee joints regardless of related symptoms in all experimental animals (23). In addition, both untreated ICR mice and asymptomatic HSV-infected mice were used as controls since only 15% of total HSV-challenged mice presented BD-like symptoms (7). According to the microPET findings and histology in this study, we found that HSV-infected, but asymptomatic mice also presented a remarkable PET-positive inflammatory process. Although the exact reason for higher FDG uptake and more intensive cellular infiltration in the joint lesions of HSV-infected asymptomatic mice than those of BD-like mice have not been elucidated, we supposed that HSV-infected asymptomatic mice could have a relatively longer disease duration between the onset of inflammatory process and microPET evaluation than symptomatic mice.

Many studies have demonstrated that FDG uptake is increased in both inflammatory tissue and tumours, demonstrating the clinical feasibility and usefulness of FDG PET in quantifying and monitoring inflammatory processes (24-29). The exact mechanism of FDG uptake is not clearly elucidated, but an increase in glycolytic activity combined with translocation of glucose transporters is a possible mechanism (30, 31). Several studies have assessed the clinical value of FDG PET in BD patients, however, most of the studies emphasised the detectability of FDG PET (10-12, 32), so the degree of FDG uptake, presumably reflecting the degree of inflammation, was not in focus. In this study, we used visual quantification of the cellular infiltrate in BD lesions to measure the severity of the lesional inflammatory process and compared it with the degree of FDG uptake on small-animal FDG PET. Statistical analysis showed that the degree of FDG uptake, represented as the proportion of injected dose (% ID/g), was significantly correlated with the severity of the inflammatory process, and our findings demonstrated the feasibility and usefulness of FDG PET for objective *in vivo* quantification of inflammation. In contrast to histopathology, FDG PET cannot differentiate the exact cellular composition of the inflammatory infiltrate. It is reported that FDG uptake is remarkably enhanced in macrophage-dense regions in chronic inflammatory tissue (25), however, research has shown that other types of white blood cells also showed variable degrees of FDG uptake, and such results seem to make accurate differentiation of the cellular components impossible (26, 33-35). The clinical efficacy of FDG PET for the evaluation of intestinal inflammation has not been evaluated in BD patients, and as shown in the present animal study, the decreased sensitivity for intra-abdominal lesions are other weak points of FDG PET due to the limitations of spatial resolution and physiologic FDG uptake in skeletal muscles and bowel.

Still, we suggest that FDG PET provides much valuable knowledge to overcome these drawbacks. First, FDG PET can detect visceral involvement of disease, even in its early or asymptomatic stage. In our study, FDG PET revealed small bowel obstruction and the probable leading point of intestinal BD involvement in one mouse. Furthermore, the degree of FDG uptake in elbow and knee joints was significantly higher in the disease group than in the control group, and histopathologic analysis confirmed the corresponding difference in the number of inflammatory cells in the synovia. This result could suggest another possible application of FDG PET as a screening tool in asymptomatic BD patients in addition to monitoring disease activity. Second, whereas histopathologic evaluation inevitably requires sacrificing animals and therefore is limited in observation of the complete disease process and response assessment of multiple interventions in a living subject, FDG PET allows for repeated investigations of the same subject even with multiple disease-modulating interventions. This advantage enables not only longitudinal analyses within the same animal, but also direct and objective comparisons of treatment responses. In addition, when compared with other *in vivo* functional imaging modalities such as optical imaging, FDG PET is still superior in depth of penetration, spatial resolution, and objective quantification. Therefore, FDG PET is suggested as an important tool to non-invasively and accurately quantifies experimental inflammation *in vivo*.

Conclusion

In conclusion, our data indicates that FDG PET can non-invasively and quantitatively detect the inflammatory process in an HSV-induced BD-like mouse model. In addition, we suggest that FDG PET can be applicable for human BD patients as well as the experimental models with the clinical values of a baseline workup study and a guidance and control of anti-inflammatory treatment.

Acknowledgments

We thank Hye Sun Lee, PhD (Department of Biostatistics, Yonsei University College of Medicine, Seoul, Korea) for her help with the statistical analyses.

References

1. SAKANE T, TAKENO M, SUZUKI N, INABA G: Behçet's disease. *N Engl J Med* 1999; 341: 1284-91.
2. EGLIN RP, LEHNER T, SUBAK-SHARPE JH: Detection of RNA complementary to herpes-simplex virus in mononuclear cells from patients with Behçet's syndrome and recurrent oral ulcers. *Lancet* 1982; 2:1356-61.
3. BEHÇET H: Über rezidivierende, aphthöse, durch ein Virus verursachte Geschwüre im Mund, am Auge und an den Genitalien. *Dermatol Wochenschr* 1937; 105: 1152-7.
4. LEE S, BANG D, CHO YH, LEE ES, SOHN S: Polymerase chain reaction reveals herpes simplex virus DNA in saliva of patients with Behçet's disease. *Arch Dermatol Res* 1996; 288: 179-83.
5. SEZER FN: The isolation of a virus as the cause of Behçet's diseases. *Am J Ophthalmol* 1953; 36: 301-15.
6. SHIMIZU J, IZUMI T, ARIMITSU N *et al*.: Skewed TGFβ/Smad signaling pathway in T cells in patients with Behçet's disease. *Clin Exp Rheumatol* 2012; 30 (Suppl. 72): S35-9.
7. SOHN S, LEE ES, BANG D, LEE S: Behçet's disease-like symptoms induced by the Herpes simplex virus in ICR mice. *Eur J Dermatol* 1998; 8: 21-3.
8. SOHN S, BANG D, LEE ES, KWON HJ, LEE SI, LEE S: Experimental studies on the antiviral agent famciclovir in Behçet's disease symptoms in ICR mice. *Br J Dermatol* 2001; 145: 799-804.
9. WEINER SM, OTTE A, SCHUMACHER M *et al*.: Neuro-Behçet's syndrome in a patient not fulfilling criteria for Behçet's disease: clinical features and value of brain imaging. *Clin Rheumatol* 2000; 19: 231-4.
10. WILDHAGEN K, MEYER GJ, STOPPE G, HEINTZ P, DEICHER H, HUNDESHAGEN H: PET and MR imaging in a neuro-Behçet syndrome. *Eur J Nucl Med* 1989; 15: 764-6.
11. DENECKE T, STAECK O, AMTHAUER H, HANNINEN EL: PET/CT visualises inflammatory activity of pulmonary artery aneurysms in Behçet's disease. *Eur J Nucl Med Mol Imaging* 2007; 34: 970.
12. CHO SB, YUN M, LEE JH, KIM J, SHIM WH, BANG D: Detection of cardiovascular system involvement in Behçet's disease using fluorodeoxyglucose positron emission tomography. *Semin Arthritis Rheum* 2011; 40: 461-6.
13. CHO SB, CHO S, LEE JH, LEE JD, BANG D: Erythema nodosum-like skin lesions associated with Behçet's disease show 18F-fluorodeoxyglucose uptake on PET/CT. *Clin Exp Rheumatol* 2011; 29 (Suppl. 67): S91-2.
14. CHO SB, YUN M, CHO S, LEE JH, LEE JH, BANG D: Visualization of the inflammatory process in Behçet's disease using fluorodeoxyglucose positron emission tomography: a case report. *Clin Exp Rheumatol* 2010; 28 (Suppl. 60): S92-3.
15. VISSER EP, DISSELHORST JA, BROM M *et al*.: Spatial resolution and sensitivity of the Inveon small-animal PET scanner. *J Nucl Med* 2009; 50: 139-47.
16. SCHUBERT D, MAIER B, MORAWIETZ, KRENN V, KAMRADT T: Immunization with glucose-6-phosphate isomerase induces T cell-dependent peripheral polyarthritis in genetically unaltered mice. *J Immunol* 2004; 172: 4503-9.
17. TALARICO R, D'ASCANIO A, FIGUS M *et al*.: Behçet's disease: features of neurological involvement in a dedicated centre in Italy. *Clin Exp Rheumatol* 2012; 30 (Suppl. 72): S69-72.
18. HAMURYUDAN V, HATEMI G, SUT N, UGURLU S, YURDAKUL S, YAZICI H: Frequent oral ulceration during early disease may predict a severe disease course in males with Behçet's syndrome. *Clin Exp Rheumatol* 2012; 30 (Suppl. 72): S32-4.
19. HATEMI G, SEYAHI E, FRESKO I, HAMURYUDAN V: Behçet's syndrome: a critical digest of the recent literature. *Clin Exp Rheumatol* 2012; 30 (Suppl. 72): S80-9.
20. KUROKAWA MS, YOSHIKAWA H, SUZUKI N: Behçet's disease. *Semin Respir Crit Care Med* 2004; 25: 557-68.
21. CHOI B, KIM J, LEE ES, BANG D, SOHN S: Synthesized pyridine compound derivatives decreased TNF alpha and adhesion molecules and ameliorated HSV-induced inflammation in a mouse model. *Eur J Pharmacol* 2011; 657: 167-72.
22. IRMLER IM, OPFERMANN T, GEBHARDT P *et al*.: *In vivo* molecular imaging of experimental joint inflammation by combined (18) F-FDG positron emission tomography and computed tomography. *Arthritis Res Ther* 2010; 12: R203.
23. BANG D, LEE JH, LEE ES *et al*.: Epidemiologic and clinical survey of Behçet's disease in Korea: the first multicenter study. *J Korean Med Sci* 2001; 16: 615-8.
24. DAVIES JR, IZQUIERDO-GARCIA D, RUDD JH *et al*.: FDG-PET can distinguish inflamed from non-inflamed plaque in an animal model of atherosclerosis. *Int J Cardiovasc Imaging* 2010; 26: 41-8.
25. KAIM AH, WEBER B, KURRER MO, GOTTSCHALK J, VON SCHULTHESS GK, BUCK A: Autoradiographic quantification of 18F-FDG uptake in experimental soft-tissue abscesses in rats. *Radiology* 2002; 223: 446-51.
26. KAIM AH, WEBER B, KURRER MO *et al*.: (18) F-FDG and (18)F-FET uptake in experimental soft tissue infection. *Eur J Nucl Med Mol Imaging* 2002; 29: 648-54.
27. OGAWA M, MAGATA Y, KATO T *et al*.: Application of 18F-FDG PET for monitoring the therapeutic effect of antiinflammatory drugs on stabilization of vulnerable atherosclerotic plaques. *J Nucl Med* 2006; 47: 1845-50.
28. RUDD JH, MYERS KS, BANSILAL S *et al*.: (18)Fluorodeoxyglucose positron emission tomography imaging of atherosclerotic plaque inflammation is highly reproducible: implications for atherosclerosis therapy trials. *J Am Coll Cardiol* 2007; 50: 892-6.
29. TAWAKOL A, MIGRINO RQ, HOFFMANN U *et al*.: Noninvasive *in vivo* measurement of vascular inflammation with F-18 fluorodeoxyglucose positron emission tomography. *J Nucl Cardiol* 2005; 12: 294-301.
30. MELLER J, SAHLMANN CO, SCHEEL AK: 18F-FDG PET and PET/CT in fever of unknown origin. *J Nucl Med* 2007; 48: 35-45.
31. PASTERNAK CA, AIYATHURAI JE, MAKINDE V *et al*.: Regulation of glucose uptake by stressed cells. *J Cell Physiol* 1991; 149: 324-31.
32. ANTHONY MP, ZHANG J, KHONG PL: PET/CT appearance of intestinal Behçet's disease. *Clin Nucl Med* 2009; 34: 825-6.
33. JONES HA, CHOUDHURY M, HARRIS DN: *In vivo* measurement of circulating leucocyte activation in patients following cardiopulmonary bypass. *Nucl Med Biol* 2004; 31: 965-9.
34. JONES HA, CLARK RJ, RHODES CG, SCHOFIELD JB, KRAUSZ T, HASLETT C: *In vivo* measurement of neutrophil activity in experimental lung inflammation. *Am J Respir Crit Care Med* 1994; 149: 1635-9.
35. PIO BS, BYRNE FR, ARANDA R *et al*.: Noninvasive quantification of bowel inflammation through positron emission tomography imaging of 2-deoxy-2-[18F]fluoro-D-glucose-labeled white blood cells. *Mol Imaging Biol* 2003; 5: 271-7.